NJC

ROYAL SOCIETY OF CHEMISTRY

PAPER

View Article Online
View Journal

Cite this: DOI: 10.1039/d0nj00052c

Dinuclear cobalt complexes supported by biphenol and binaphthol-derived bis(salicylaldimine) ligands: synthesis, characterization and catalytic application in β-enaminone synthesis from 1,3-dicarbonyl compounds and aliphatic amines†

Adelew Estifanos Filkale *[a] and Chandni Pathak [b]

Two new tetradentate ligands, namely, 3,3′-bis[((2,4,6-trimethyl-phenyl)imino)methyl]-[1,1′]-biphenyl-2,2′-diol, H_2L^1 (**1**), and 3,3′-bis[((2,4,6-trimethylphenyl)imino)methyl]-[1,1′]-binaphthalenyl-2,2′-diol, H_2L^2 (**3**), based on 2,2′-biphenol and 2,2′-binaphthol frameworks have been synthesized and characterized. Correspondingly, dinuclear cobalt complexes {Co[3,3′-bis-((R)-iminomethyl)-(1,1′)-biphenyl-2,2′-dioxo]}$_2$ (**2**) and {Co[3,3′-bis-((R)-iminomethyl)-(1,1′)-binaphthalenyl-2,2′-dioxo]}$_2$ (**4**) (where R = 2,4,6-$Me_3C_6H_2$) were synthesized *via* reactions of the respective ligands with tetrahydrate cobalt acetate. The complexes were then characterized by elemental analysis, mass spectrometry, IR, UV-vis, magnetic susceptibility and single-crystal X-ray diffraction analysis. The single-crystal X-ray crystallographic study indicates a distorted tetrahedral geometry for each of the metal ions in **2** and **4**. The magnetic susceptibility measurements at varying temperatures (5–300 K) showed that the complexes exhibit weak anti-ferromagnetic (AF) interactions. Both metal complexes **2** and **4** successfully catalysed the synthesis of β-enaminones from 1,3-dicarbonyl compounds and aliphatic amines under ambient conditions.

Received 4th January 2020,
Accepted 28th July 2020

DOI: 10.1039/d0nj00052c

rsc.li/njc

Introduction

Transition metal complexes containing two or more metal ions possess useful characteristics and potential applications in molecular magnetism,[1,2] bio-inorganic chemistry,[1] homogeneous catalysis[3] and asymmetric synthesis.[1,3–12] In line with this, significant efforts have been directed towards the synthesis of dinucleating ligands, capable of holding two separated transition metal ions, either the same or different, which are subject to control by an appropriate modification of the molecular topology.[1,8,10,13–15] Using polydentate ligands, which possess N and O donors, has always been a wise choice to construct versatile multinuclear architectures because of their rich coordination patterns, and steric and electronic effects.[2] We have recently synthesized new homodinuclear cobalt complexes using N and O donor ligands derived from 2,2′-binaphthol and 2,2′-biphenol frameworks and studied their catalytic roles in the synthesis of β-enaminones from 1,3-dicarbonyl compounds and aliphatic amines. 2,2′-Binaphthol and 2,2′-biphenol-based ligands and complexes thereof have widespread importance in catalysis, associated with their high dinucleating capability, low toxicity and high efficiency.[11,16–21] On the other hand, cobalt complexes have attracted much attention as a promising alternative catalyst for enaminone synthesis and other varieties of organic reactions due to the low price, interesting reactivity, non-toxicity and environmentally well-suited character of cobalt.[13,18,22,23]

Enaminones are widely used as versatile building blocks for the synthesis of important bioactive heterocyclic compounds and different biologically active compounds.[24,25] Owing to the biologically and synthetically significant roles of β-enaminones, considerable efforts have been made for their synthesis.[25,26] However, in these procedures, the long reaction time, high reaction temperatures, use of an expensive catalyst,[27] high catalyst loading, unsatisfactory yields, and use of an additional microwave oven and ultrasound have imposed

[a] Department of Chemistry, College of Computational & Natural Sciences, Hawassa University, P. O. Box, 05, Ethiopia.
E-mail: adelewshenkora@gmail.com, adelew@hu.edu.et
[b] Department of Applied Chemistry, Jabalpur Engineering College, Jabalpur, M. P., India

† Electronic supplementary information (ESI) available: ^{1}H NMR, ^{13}C{^{1}H} NMR, IR, HRMS, and elemental analysis data of 3,3′-bis[(2,4,6-trimethyl-phenylimino)-methyl]-[1,1′]biphenyl-2,2′-diol (H_2L^1), 3,3′-bis[(2,4,6-trimethyl-phenylimino)-methyl]-[1,1′]binaphthalenyl-2,2′-diol (H_2L^2) and the dinuclear cobalt complexes **2** and **4**, the CIF file giving X-ray crystallographic, ^{1}H NMR, ^{13}C{^{1}H} NMR, GC-MS chromatogram and elemental analysis data of the catalysis products and table of optimization (time, solvent, catalyst) results can be found on the journal webpage.CCDC 960053 and 979501. For ESI and crystallographic data in CIF or other electronic format see DOI: 10.1039/d0nj00052c

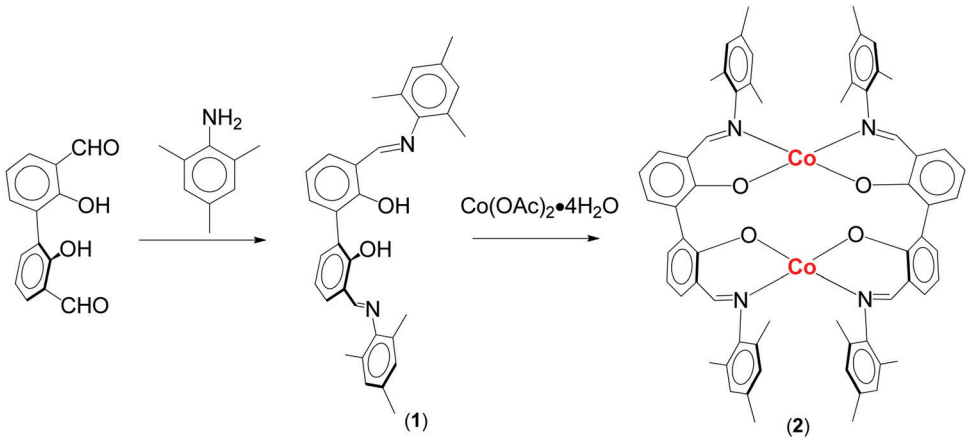

Scheme 1 Synthesis of the homodinuclear cobalt $[CoL^1]_2$ (**2**) complex supported by a 2,2′-biphenol based salen type ligand (**1**).

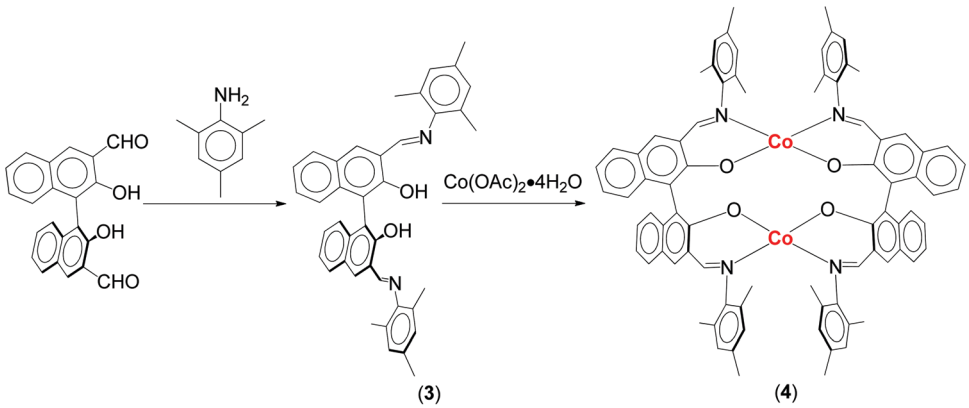

Scheme 2 Synthesis of the homodinuclear cobalt $[CoL^2]_2$ (**4**) complex supported by a 2,2′-binaphthol (R-BINOL) based salen type ligand (**3**).

limitations on large-scale applications in organic synthesis.[25–30] In this respect, the development of inexpensive, easily available and non-toxic catalysts is highly attractive for chemical synthesis.[25,31] Herein we report the synthesis, crystal structure and catalytic activities of new homodinuclear cobalt(II) complexes {Co[3,3′-bis-((R)-iminomethyl)-(1,1′)-biphenyl-2,2′-dioxo]}$_2$ (**2**) and {Co[3,3′-bis-((R)-iminomethyl)-(1,1′)-binaphthalenyl-2,2′-dioxo]}$_2$ (**4**). Each Co(II) center within the dinuclear complex cations shown in Schemes 1 and 2 has tetradentate cavities coordinated to two N and two O sites, leaving the metal center coordinatively unsaturated, and thus room for further coordination[22] by exogenous ligands. In contrast to **4**, complex **2** exhibited better catalytic activity towards a variety of 1,3-dicarbonyl compounds and aliphatic amines. To the best of our knowledge, complexes **2** and **4** are the first examples of dinuclear cobalt complexes which have been synthesised, structurally characterized and evaluated as catalysts in β-enaminone synthesis from 1,3-dicarbonyl compounds and aliphatic amines.

Results and discussion

Synthesis of the complexes

Red crystalline dinuclear cobalt(II) complexes of the type {Co[3,3′-bis-((R)-iminomethyl)-(1,1′)-biphenyl-2,2′-dioxo]}$_2$ (**2**) and {Co[3,3′-bis-((R)-iminomethyl)-(1,1′)-binaphthalenyl-2,2′-dioxo]}$_2$ (**4**), R = 2,4,6-$Me_3C_6H_2$,[5] were synthesized by the treatment of a hot methanolic solution of the corresponding ligand with a hot methanolic solution containing $Co(OAc)_2{\cdot}4H_2O$ in 22 and 20% yields, respectively. The ligands $\mathbf{H_2L^1}$ (**1**) and $\mathbf{H_2L^2}$ (**3**) were generated in a four step reaction from commercially available racemic biphenol and optically pure R-binol precursors, respectively.[21,32] The dideprotonated species $\mathbf{H_2L^1}$ (**1**)/$\mathbf{H_2L^2}$ (**3**) acted as N_2O_2 donor-tetradentate ligands in which the two cobalt(II) ions are sandwiched between the two tetradentate ligands.[33]

Both complexes **2** and **4** are thermally stable, and air and moisture insensitive on storage under ordinary conditions, exhibiting good solubility in common nonpolar organic solvents, but are slightly soluble in polar solvents like methanol. The molecular identity and geometry of both complexes were elucidated by X-ray crystal structure determination. ESI-MS analysis and satisfactory analytical data on crystalline materials demonstrate the purity of both compounds.

UV-vis spectra of the ligands and complexes

The UV-visible absorption spectra of the ligands ($\mathbf{H_2L^n}$) and complexes (**2** and **4**) measured in CH_2Cl_2 solutions at room temperature are shown in Fig. 1. The electronic spectra of the

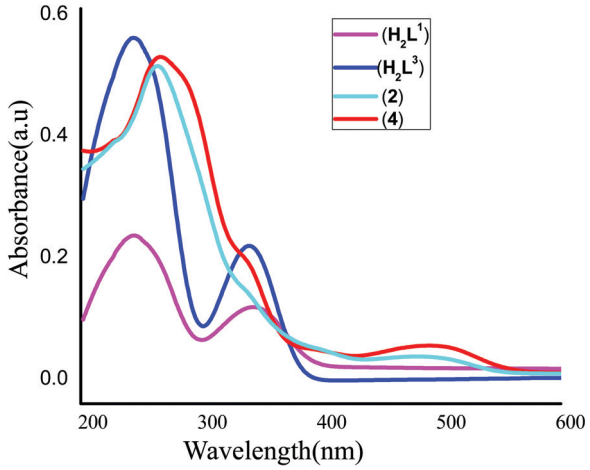

Fig. 1 UV-visible spectra of **1**, **2**, **3**, and **4** ([C] = 1×10^{-3} M) in CH_2Cl_2 at 25 °C.

free ligands show two strong absorption bands in the UV-vis regions 200–300 and 300–400 nm, which can be attributed to the π → π* and n → π* transitions, respectively.[8,34,35] Upon complex formation with Co(II) ions, the bands which were characteristic of the free ligands are red shifted to 330–336 nm (π → π*) and 250–290 nm (n → π*) in complex **2** and 390–430 nm (π → π*) and 240–277 nm (n → π*) in complex **4**. This can be attributed to the rigidity, which was enhanced after the ligand coordination with the Co(II) ion, and so the energy required for an electron transition from the ground state to the excited state is reduced.[36] Consequently, the absorption of the $\mathbf{H_2L^n}$ ligands is red shifted after coordination with Co(II) ions. In addition, a new band located around 440–550 nm appears in the spectra of the complexes.[8,34,35] This new band is attributed to the d → π* charge transfer transition, which can be assigned as MLCT (Metal Ligand Charge Transfer). In some cases the n → π* transition is not fully visible and instead forms a poorly resolved shoulder in the spectra of the complexes as it may overlap with the charge transfer (d → π* or π* → d) transitions.[37] These alterations in shifts and intensity for the absorption bands support the coordination of the ligand to the M(II) ion. The differences in the intensity of absorption, band shape, shifts and number of bands of the complexes and ligands are visible and easier to compare as shown in Fig. 1. The complexes show no apparent bands within the 900–600 nm range at the given concentration ([C] = 1×10^{-3} M), although it is very likely that the expected d–d electronic transitions are masked by the very broad and intense charge transfer bands as reported for known Co(salen) complexes.[37]

Single crystal X-ray diffraction analysis

Red crystals of **2** and **4** suitable for single crystal X-ray crystallographic analysis were obtained by slow evaporation of the complex solution in dichloromethane–acetonitrile (1 : 1) at room temperature. The single crystal X-ray diffraction data and experimental details for complexes **2** and **4** are available in Table 1 and selected bond parameters are summarized in Table 2. The crystal

Table 1 X-ray crystallographic data for **2** and **4**

Compound	**2**	**4**
Lattice	Monoclinic	Monoclinic
Formula	$C_{64}H_{60}Co_2N_4O_4$	$C_{80}H_{68}Co_2N_4O_4$
Formula weight	1066.33	1267.25
Space group	$P2_1/n$	$P2_1$
a/Å	17.899(5)	15.965(5)
b/Å	13.249(5)	12.533(5)
c/Å	24.649(5)	20.132(5)
α/°	90	90
β/°	90	111.862(5)
γ/°	90	90
V/Å	5845(3)	3739(2)
Z	4	4
Temperature (K)	150	150
Radiation (λ, Å)	0.71073	0.71073
ρ (calcd), g cm^{-3}	1.306	1.126
θ max, deg.	25.000	25.000
No. of data	10 298	6907
No. of parameters	745	812
R_1	0.0516	0.0652
wR_2	0.1292	0.1799
GOF	1.144	1.052

Table 2 Selected bond distances (Å) and angles (deg.) for compounds **2** and **4**

2		**4**	
N(1)–Co(1)	1.996(2)	N(1)–Co(1)	1.986(3)
N(2)–Co(1)	1.995(2)	N(2)–Co(1)	1.991(3)
N(3)–Co(2)	1.997(2)	N(3)–Co(2)	2.015(3)
N(4)–Co(2)	1.999(2)	N(4)–Co(2)	2.017(3)
O(1)–Co(1)	1.911(2)	O(1)–Co(1)	1.899(3)
O(2)–Co(2)	1.9119(19)	O(2)–Co(1)	1.907(3)
O(3)–Co(1)	1.912(2)	O(3)–Co(2)	1.935(3)
O(4)–Co(2)	1.917(2)	O(4)–Co(2)	1.890(3)
O(1)–Co(1)–O(3)	112.73(9)	O(1)–Co(1)–O(2)	116.80(13)
O(1)–Co(1)–N(1)	94.55(9)	O(1)–Co(1)–N(1)	95.63(11)
O(3)–Co(1)–N(1)	123.72(9)	O(2)–Co(1)–N(1)	115.63(14)
O(1)–Co(1)–N(3)	119.23(9)	O(1)–Co(1)–N(2)	117.41(12)
O(3)–Co(1)–N(3)	94.79(9)	O(2)–Co(1)–N(2)	95.15(11)
N(1)–Co(1)–N(3)	113.88(9)	N(1)–Co(1)–N(2)	117.90(13)
O(2)–Co(2)–O(4)	114.07(9)	O(4)–Co(2)–O(3)	122.27(12)
O(2)–Co(2)–N(2)	94.58(9)	O(4)–Co(2)–N(3)	110.71(12)
O(4)–Co(2)–N(2)	121.92(9)	O(3)–Co(2)–N(3)	94.05(11)
O(2)–Co(2)–N(4)	119.81(9)	O(4)–Co(2)–N(4)	93.32(12)
O(4)–Co(2)–N(4)	94.86(9)	O(3)–Co(2)–N(4)	121.00(11)
N(2)–Co(2)–N(4)	113.65(10)	N(3)–Co(2)–N(4)	116.99(12)

Symmetry codes: (**2**) 1/2 − X, 1/2 + Y, 1/2 − Z; (**4**) −X, 1/2 + Y, −Z

structures of the complexes together with the corresponding atom-labeling schemes of **2** and **4** are presented in Fig. 2 and 3. Complexes **2** and **4** are isomorphous and crystallize in the monoclinic space groups $P2_1/n$ and $P2_1$, respectively. The dinuclear cobalt(II) complexes **2** and **4** involve two Co(II) ions bridging the two ligand systems through two fold coordination of the phenolate-O and azomethine-N. The intra-dimer Co···Co distances were 5.19(7) Å (**2**) and 5.10(7) Å (**4**). Both Co1 and Co2 are tetra coordinated, being surrounded by two adjacent imine-N and two biphenolate-O atoms of the ligands.[18]

The coordination geometry is distorted considerably from tetrahedral, as can be seen by calculating the τ_4 index.

This metric was proposed by Yang *et al.*[38] as a method for qualitatively evaluating the geometry of four-coordinate complexes.

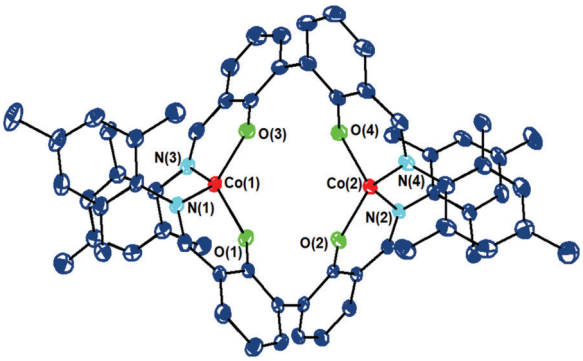

Fig. 2 ORTEP of **2** with thermal ellipsoids drawn at the 50% probability level. All hydrogen atoms are omitted for clarity.

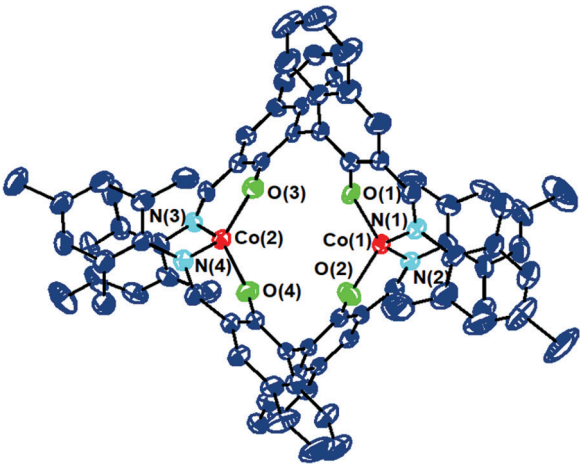

Fig. 3 ORTEP of **4** with thermal ellipsoids drawn at the 50% probability level. All hydrogen atoms are omitted for clarity.

$$\tau_4 = 360 - (\alpha + \beta)/141^\circ$$

α and β are the two largest angles subtended by the ligand donor atoms in the four-coordinate complex.

The average indexes for **2** and **4** were found to be 0.83 and 0.86, respectively, signifying a considerable distortion from an idealized tetrahedral, T_d, geometry ($\tau_4 = 1.0$) towards a seesaw C_{2v} configuration. The distortion from a regular tetrahedron is remarkable in the geometries of the X-ray structure of dicobalt complex **4** in the angle formed by O(1)–Co(1)–N(1) 95.63°, which is much smaller than the regular tetrahedral angle, while the angle O(1)–CO(1)–N(2) 117.4° is remarkably large (Table 2).[39]

For each Co(II) ion, the two oxygen atoms come from the deprotonated biphenol-O atom and two nitrogen atoms from the imine–N atom of the ligand. The Co–O and Co–N bond lengths are in the respective ranges 1.911(2)–1.919(19) and 1.995(2)–2.017(3) Å for the two complexes, comparable to similar systems.

Magnetic susceptibilities

Magnetic susceptibility measurements for the dicobalt complexes were made on polycrystalline samples in the range of 5–300 K. The temperature dependence of χ_M, $\chi_M T$ and χ_M^{-1} per two Co(II) for **2** is shown in Fig. 4 and 5, respectively.

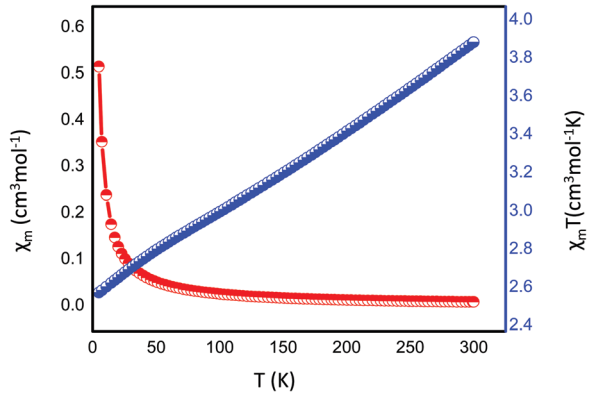

Fig. 4 Temperature dependence plot of χ_M and $\chi_M T$ for complex **2** at 100 Oe. The solid line represents the best fit curve.

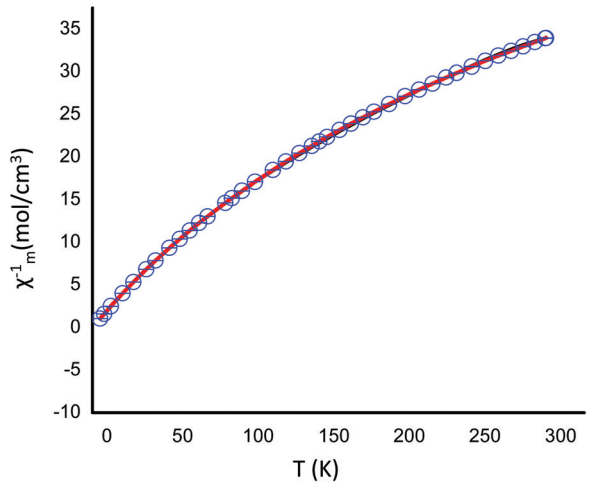

Fig. 5 Temperature dependence plot of $1/\chi_M$ for complex **2** at 100 Oe. The solid line represents the best fit curve.

The complex shows significant temperature dependence of the magnetic susceptibility, although the behaviour differs upon cooling.[10] The $\chi_M T$ values vary from 2.61 to 3.90 cm^{-3} mol^{-1} K in the range 5–300 K for **2**. The obtained $\chi_M T$ value at room temprature is closer to the spin-only value calculated for two non-interacting high spin cobalt(II) ions (3.75 cm^{-3} mol^{-1} K with $S = 3/2$ and $g = 2.0$),[40,41] which show small spin–orbit coupling[6,42] (Table 3). This fact is in accordance with the general conclusion for Co^{2+} ions in tetrahedral crystal fields.[43] The magnetic studies show that the cobalt(II) ions in **2** are high spin, expected for low symmetry four coordinated environments ($S = 3/2$).[44] The plot of χ_M^{-1} *vs.* T for **2** (Fig. 5) followed Curie–Weiss behaviour in the temperature range of 50–300 K, where $1/\chi_M = (1/C)T + \theta/C$.[9,45] Accordingly, for complex **2** the molar Curie constant $C = 4.72$ mol cm^{-3} K and Weiss temperature $\theta = -6.8$ K (x-intercept) were obtained.[23,46] The negative value of the Weiss constant indicates the presence of weak antiferromagnetic interaction in the dinuclear cobalt(II) complex **2**. Upon cooling, the $\chi_M T$ value decreases steadily to a minimum of 2.61 cm^{-3} mol^{-1} K at 6 K. Generally, the decrease in the magnitude of $\chi_M T$ with decreasing system temperature

Table 3 Magnetic data for **2** and **4** at 300 K

S. no.	Metal complex	Obs. χ_M ($cm^3\ mol^{-1}$)	$1/\chi$ ($cm^3\ mol^{-1}$)	$\chi_M T$ ($cm^3\ mol^{-1}\ K$)	$\mu_{ss}{}^a$ (B)	$\mu_{LS}{}^b$ (B)	Obs. μ_{eff} (μ_B)
1	**2**	0.014	75	3.9	5.4	7.3	5.6
2	**4**	0.018	90.9	4.0	5.4	7.3	5.7

^{a} $\mu_{ss} = [g_i{}^2 S_i(S_i + 1)]^{1/2}$, with $S = 3/2$ for a hs Co(II). ^{b} $\mu_{LS} = [\sum L_i(L_i + 1) + \sum g_i{}^2(S_i + 1)]^{1/2}$, where $L = 3$ and $S = 3/2$ for a hs Co(II).

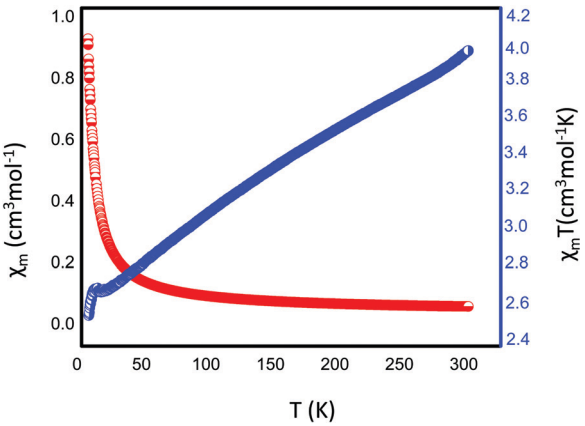

Fig. 6 Temperature dependence plot of χ_M and $\chi_M T$ for complex **4** at 100 Oe. The solid line represents the best fit curve.

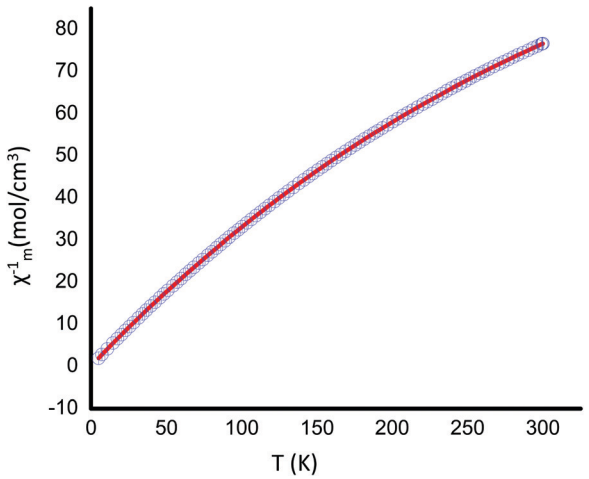

Fig. 7 Temperature dependence plot of $1/\chi_M$ for complex **4** at 100 Oe. The solid line represents the best fit curve.

for these types of complexes could result from several factors such as the partial depopulation of excited magnetic states,[40] zero-field splitting effects, and significant spin–orbit coupling due to mixing of ground and excited states inherent to the Co(II) ions, as well as non-negligible intermolecular interactions, even at room temperature.[42,47] Complex **4** also showed significant temperature dependence of the magnetic susceptibility, although upon cooling the behaviour differs from that of complex **2**. As illustrated in Fig. 6, the measured $\chi_M T$ value at 300 K is about 4.0 $cm^3\ K\ mol^{-1}$, which is in accordance with the $\chi_M T$ value of two isolated high spin cobalt(II) ions (3.75 $cm^{-3}\ mol^{-1}\ K$ with $S = 3/2$ and $g = 2.0$) (Table 3). The small deviation of the calculated magnetic susceptibility from the experimental value may be caused by paramagnetic impurities. These impurities might tilt the structure and cause the increase/decrease of the magnetic susceptibility.[5] The $\chi_M T$ value decreases smoothly to 50 K with values from 4.0 to 2.5 $cm^3\ K\ mol^{-1}$ as the system temperature decreases and then abruptly decreases below 25 K, reaching a minimum value of 1.09 $cm^3\ K\ mol^{-1}$ at 5.0 K. The sharper decrease below 25 K may be attributed to depopulation of the crystal field split energy levels (zero field splitting) and/or antiferromagnetic intermolecular interactions.[41]

It is possible, though unlikely, that the decrease in $\chi_M T$ upon cooling might be due to an incomplete spin crossover transition to a low spin cobalt(II) ion; an example with an N_4O_2 coordination sphere has been reported.[41]

The plot of $\chi_M{}^{-1}$ *vs.* T above 25 K (Fig. 7) obeys Curie–Weiss behaviour, which could give $C = 4.85\ cm^3\ K\ mol^{-1}$ and $\theta = -12.15$ K. The negative Weiss constant indicates the existence of an antiferromagnetic interaction in dinuclear complex **4**.

An isotropic spin Hamiltonian equation $\hat{H} = -2JS_1S_2$ (where J = exchange integral between cobalt ions) was used to account for intramolecular magnetic interactions.[48,49] We explored the dimer model employed for analogous complexes,[43] considering $S_1 = S_2 = 3/2$.

The best possible fitting was obtained for **2** with an isotropic coupling constant $J_{CoCo} = -5\ cm^{-1}$ and $g_{CoCo} = 1.99$, assuming a temperature-independent paramagnetic correction of $N\alpha = 1.40 \times 10^{-5}\ cm^3\ mol^{-1}$, magnetic impurity (MI) = 0.36% (Table 4).

Similarly, the best agreement with the experimental data was obtained for **4** with $J_{CoCo} = -6.5\ cm^{-1}$ and $g_{CoCo} = 1.99$, assuming a temperature-independent paramagnetic correction of $N\alpha = 2.81 \times 10^{-3}\ cm^3\ mol^{-1}$, magnetic impurity (MI) = 0.83% (Table 4).

The negative J values confirm the presence of weak antiferromagnetic interactions between the Co(II) ions in both **2** and **4**.[13,50] The antiferromagnetic coupling observed in the complexes may be explained from the magneto-structural correlations established for binaphthol and biphenol linkers.[51] These correlations established that the magnetic coupling strongly depends on the Co–O, Co–N and Co···Co separation and to a small extent on the geometries around the coupling.[23,49] In the present case, the exchange coupling (J) may be explained in terms of both the Co···Co distance and the geometrical distortions that affect the cobalt coordination spheres.[40] However, more examples of similar dicobalt(II) complexes are needed to establish the relationship between the structure and the nature of the magnetic coupling between the high-spin cobalt(II) ions.

ESI mass spectrometry

The mass spectrometric data of positive ions $[M]^+$ corresponding to the complexes were evidenced by ESI† using $CHCl_3$ as a solvent and the ESI-mass spectra are shown in the ESI.†

Table 4 List of magnetic fitting parameters in complexes **2** and **4**

S. no.	Metal complex	$g_{co(II)}$	J_{CoCo} (cm^{-1})	Temperature independent paramagnetism (10^{-3} cm^3 mol^{-1})	Magnetic impurity (%)
1	**2**	1.99	−5	1.40	0.36
2	**4**	1.99	−6.5	2.51	0.83

The spectrometric data of complex **2** show a peak at m/z = 1067.3346. This peak can be assigned to $[C_{64}H_{60}Co_2N_4O_4]^+$ (calc. 1067.3351) (ESI,† Fig. S8). For complex **2**, there is another peak at m/z = 1089.3164 which may correspond to species of formula $[C_{64}H_{60}Co_2N_4NaO_4]^+$ (calc. m/z = 1089.3171). The mass spectra of complex **4** contain a base peak at m/z = 1267.3919 which can be assigned to $[C_{80}H_{69}Co_2N_4O_4]^+$ (**4**) (calc. 1267.3977) (ESI,† Fig. S18). For complex **4**, there are additional m/z peaks at 1266.5571, 1268.4081, 1269.4155, and 1270.4155 corresponding to the different isotopes of the constituent atoms. The measured molecular masses of both complexes were in accord with the elemental analyses results.

Dinuclear $[CoL^1]_2$ (2) and $[CoL^2]_2$ (4) complex mediated synthesis of β-enaminones from 1,3-dicarbonyl compounds and aliphatic amines. The catalytic activities of the new dinuclear $[CoL^1]_2$ (**2**) and $[CoL^2]_2$ (**4**) complexes were evaluated in the synthesis of β-enaminones from the condensation reaction of various acyclic and cyclic 1,3-dicarbonyl compounds and aliphatic amines[52] at room temperature using THF as a solvent (Scheme 3). Significantly enough the β-enaminone product yields show a substantial increase of *ca.* 51% (**2**) and of *ca.* 47% (**4**) for the representative substrates, acetyl acetone and methyl amine, when compared with the control run performed with $Co(OAc)_2{\cdot}4H_2O$ under analogous reaction conditions. The dinuclear $[CoL^1]_2$ (**2**) and $[CoL^2]_2$ (**4**) complexes showed significant enhancement in the β-enaminone product yields when compared to the blank run, which showed only *ca.* 40% for the same substrate under similar reaction conditions (Table S3, ESI†).

The dinuclear $[CoL^1]_2$ (**2**) and $[CoL^2]_2$ (**4**) complexes effectively accomplished the condensation reaction between pentane-2,4-dione and a variety of amines like methyl amine, ethyl amine, *n*-propyl amine, isopropyl amine, *n*-butyl amine and 2-(aminomethyl)pyridine yielding β-enamino ketones (5–10) in good to excellent yields (*ca.* 86–98%) under ambient conditions at room temperature (Table 5). The dinuclear $[CoL^1]_2$ (**2**) and $[CoL^2]_2$ (**4**) complexes also effectively carried out the condensation reaction between a cyclic 1,3-dicarbonyl compound, namely ethyl 2-oxocyclopentane-1-carboxylate, and various amines like ethylamine, *n*-propyl amine, isopropyl amine, *n*-butyl amine and 2-(aminomethyl)pyridine yielding β-enamino esters (11–14) in moderate to high yields (*ca.* 68–80%) under ambient conditions at room temperature (Table 5).

In the condensation reaction of an acyclic 1,3-dicarbonyl compound and various amines the highest yield of 98% was displayed by *n*-propyl amine as catalysed by $[CoL^1]_2$ (**2**) (Table 5, entry 3) and ethyl amine displayed the highest yield of 96% as catalysed by $[CoL^2]_2$ (**4**) (Table 5, entry 2). Similarly in the case of cyclic 1,3-dicarbonyl compound ethyl 2-oxocyclopentane-1-carboxylate, ethyl amine showed the highest yield of 77–80% as catalysed by $[CoL^1]_2$ (**2**) and $[CoL^2]_2$ (**4**) (Table 5, entry 7). It is clear from the catalytic data that complex $[CoL^1]_2$ (**2**) showed superior catalytic activity as compared to $[CoL^2]_2$ (**4**). This may be explained in terms of the ligand size. The binapthol based ligand (**3**) is relatively bulkier, which may cause steric hindrance (Scheme 4) for the approach and binding of the substrate to the metal cores in the complex and result in a slightly lower yield.

Generally, the electronic properties of the cyclic β-diketo substrates appeared to slightly influence the reactivity.[25] The results show that cyclic β-diketo substrates containing electron-donating groups like ethoxyl (Table 5, entries 7–10) give the corresponding products in lower yields. The double bond stereochemistry of all products had a Z configuration, as proved by the chemical shift of the hydrogen of the –NH group ($\delta \sim 8.63$ ppm), which strongly suggests the presence of an intramolecular hydrogen bond, stabilizing the products.

In all cases, the reactions proceeded rapidly and smoothly at room temperature compared to the methods available in the literature.

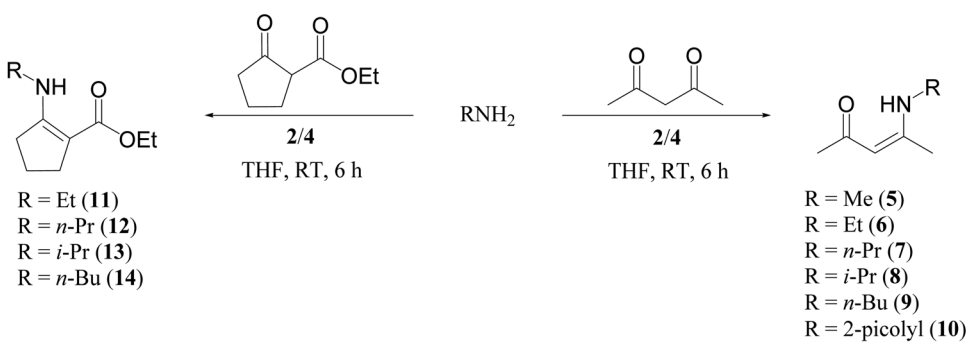

Scheme 3 General equation for β-enaminone synthesis from acyclic and cyclic β-diketo substrates with primary amines as catalysed by the dinuclear $[CoL^1]_2$ (**2**) and $[CoL^2]_2$ (**4**) complexes.

Table 5 Selected results for the β-enaminone reaction of various ketones and amines as catalyzed by the dinuclear $[CoL^1]_2$ (**2**) and $[CoL^2]_2$ (**4**) complexes[a]

S. no.	Ketone	Amine	Product	2 Yield[b]	4 Yield[b]
1	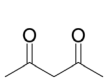	Me–NH_2	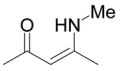 (**5**)	93	89
2	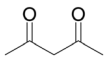	Et–NH_2	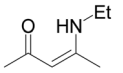 (**6**)	95	96
3	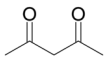	*n*-Pr–NH_2	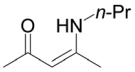 (**7**)	98	87
4	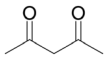	i-Pr–NH_2	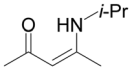 (**8**)	95	86
5	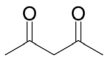	*n*-Bu–NH_2	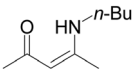 (**9**)	97	91
6	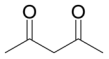	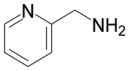	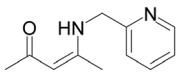 (**10**)	96	87
7	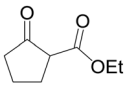	Et–NH_2	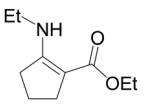 (**11**)	80	78
8	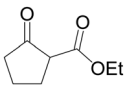	*n*-Pr–NH_2	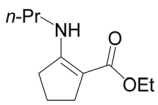 (**12**)	73	68
9	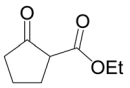	i-Pr–NH_2	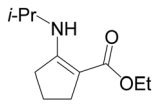 (**13**)	71	72
10	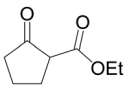	*n*-Bu–NH_2	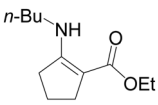 (**14**)	79	77

[a] Reaction conditions: 1.00 mmol of ketone, 4.0 mmol of amine, 1 mol% of catalyst (**2**/**4**), 2.5 mL of THF at room temperature, stir for 6 h. [b] Isolated yields (%).

A mercury poisoning experiment was performed to confirm whether the catalysis was homogeneous or heterogeneous.[53] Poisoning of any heterogeneous catalyst will inhibit the activity of the catalyst and therefore this experiment can be used as an indicator of whether or not heterogeneous catalysis is taking place.[54] Mercury(0) can form amalgams in the presence of metal particles which are responsible for heterogeneous catalysis, and this decreases the yield of the product, suppressing the activity of the catalyst. In this particular catalysis, the yield of the product was not significantly affected in the presence of mercury (Table S3, ESI,† entries 1 and 2), indicating the homogeneity of the catalysis.

The yield of enaminones in the presence of dinuclear complexes **2** and **4** was almost double as compared to the control run done with cobalt acetate tetrahydrate ($Co(OAc)_2 \cdot 4H_2O$) (Table S3, ESI†). The higher activity of the dinuclear complexes may be explicated in a manner that when the organic moiety (diketones or amines) interacts with one of the Co centers, a similar reaction could also occur at the second Co center or the second Co center participates by stabilizing reactive Co species. Of course, the increased yield may also be due to one Co center, and not two, and the fact that the ligand stabilizes the Co center in comparison to the simple salt. Consequently, structural effects and composition effects in the dinuclear complexes play an important part in their enhanced catalytic performance.

Based on the observations discussed above and the literature,[30,55–57] a plausible dinuclear $[CoL^1]_2$ (**2**) and $[CoL^2]_2$ (**4**) catalyzed reaction mechanism for the condensation reaction was proposed in Scheme 4. The condensation product generally forms through an addition–elimination reaction. The enamination reaction requires the nucleophilic addition of an amine to the carbonyl group mediated by Lewis acid centres such as {Co[3,3′-bis-((R)-iminomethyl)-(1,1′)-biphenyl-2,2′-dioxo]}$_2$ (**2**) and {Co[3,3′-bis-((R)-iminomethyl)-(1,1′)-binaphthalenyl-2,2′-dioxo]}$_2$ (**4**) (where R = 2,4,6-$Me_3C_6H_2$) complexes. Therefore, the dinuclear $[CoL^1]_2$ (**2**)/$[CoL^2]_2$ (**4**) co-ordinate to the carbonyl oxygen of the enol form of the diketone (the enol form of the diketone is more stable),[41,55] followed by the nucleophilic addition of amine. This generates a tetrahedral intermediate **E** after passing through transition states **C** and **D**, which further undergoes a water elimination reaction to yield the imine moiety. The final product β-enaminones **G** form after the tautomerization of the imine intermediate **F**.

The dinuclear $[CoL^1]_2$ (**2**) or $[CoL^2]_2$ (**4**) play an important role in catalyzing/activating the reaction by properly binding or co-ordinating with the organic substrate, resulting in the lowering of the energy barrier required for all the intermediate steps in the formation of β-enaminones. A similar observation has previously been documented for the binding of transition metal complexes on organic substrates.[55]

Conclusion

In summary, we have synthesized and characterized the first examples of homodinuclear cobalt(II) complexes **2** and **4** derived from the tetradentate ligands 3,3′-bis[((2,4,6-trimethyl-phenyl)-imino)methyl]-[1,1′]-biphenyl-2,2′-diol, $\mathbf{H_2L^1}$ (**1**), and 3,3′-bis[((2,4,6-trimethylphenyl)imino)methyl]-[1,1′]-binaphthalenyl-2,2′-diol, $\mathbf{H_2L^2}$ (**3**), respectively. The molecular structures of the

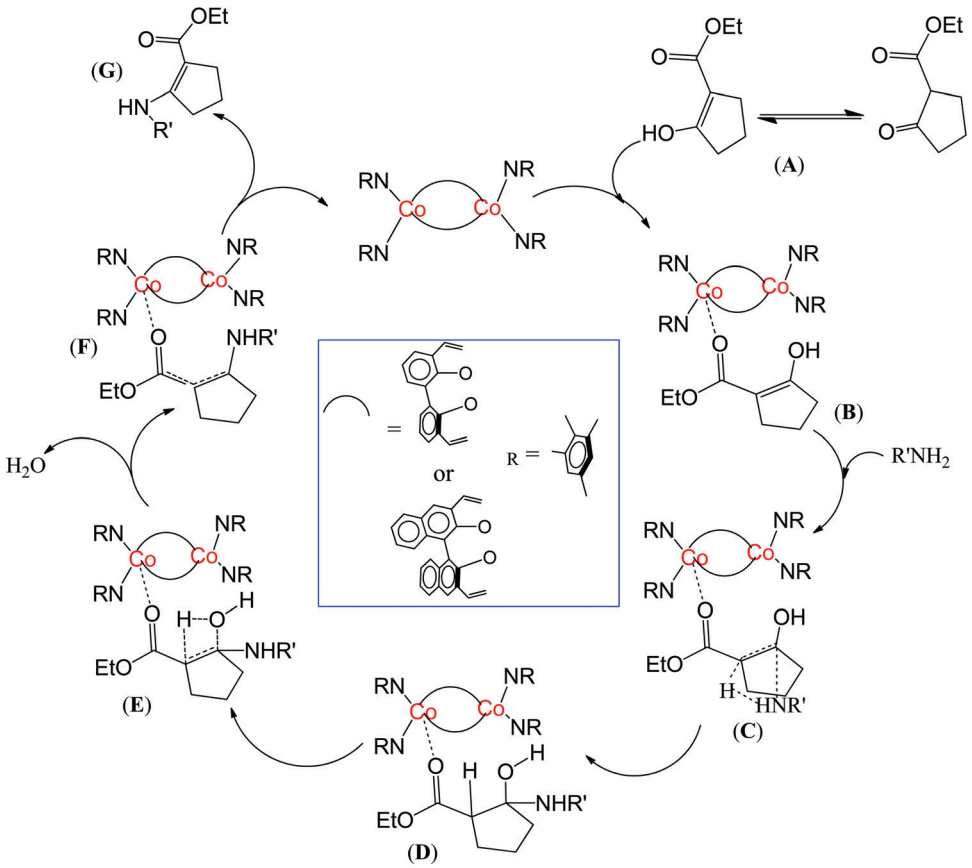

Scheme 4 Plausible mechanism for dinuclear $[CoL^1]_2$ (**2**) and $[CoL^2]_2$ (**4**) complex mediated synthesis of β-enaminones.

complexes have been determined by single-crystal X-ray crystallography at 150 K. The X-ray structures revealed a distorted tetrahedral environment in which each Co(II) center bridges the two ligand systems through two fold coordination of the phenolate-O and azomethine-N. The complexes exhibit weak antiferromagnetic coupling. Both cobalt(II) complexes demonstrated high catalytic activity towards the synthesis of β-enaminones from 1,3-dicarbonyl compounds and aliphatic amines under ambient conditions. Complex **2** revealed slightly better catalytic activity than complex **4**, which might show the influence of the ligand nature on the activity of the present dinuclear complexes. The easy and relatively low cost of preparation, and mild reaction conditions with high selectivities of the products make this a very useful catalytic system for the synthesis of β-enaminones from 1,3-dicarbonyl compounds and aliphatic amines.

Experimental

Materials and methods

General methods. Solvents were purified and degassed by standard procedures. 2,4,6-Trimethylaniline and *n*-BuLi were purchased from Sigma Aldrich (USA) and used without further purification. 2,2′-Dihydroxy-[1,1′]biphenyl-3,3′-dicarbaldehyde[58–60] and 3,3′-diformyl-2,2′-dihdroxy-1,1′-binaphthyl[18,61] were synthesized according to literature procedures. ^{1}H and ^{13}C{^{1}H} NMR spectra were recorded on Bruker 400 MHz and Bruker 500 MHz NMR spectrometers. Infrared spectra were recorded on a PerkinElmer Spectrum One FT-IR spectrometer. Mass spectrometry measurements were done on a Micromass Q-Tof and Bruker Maxis Impact spectrometer. Elemental analysis was carried out on a Thermo Quest FLASH 1112 SERIES (CHNS) elemental analyzer.

Catalytic procedures

For the catalysis runs, the GCMS analyses were done using Agilent Technologies 7890A GC systems with a 5975C inert XL EI/CI MSD Triple-Axis detector. The catalytic reactions were monitored by TLC on 0.2 mm silica gel F-254 plates. All the reaction products are known compounds and have been identified by comparing their physical and spectral characteristics with the literature reported values.

Crystallographic measurements. X-ray diffraction data for compounds **2** and **4** were collected on a Rigaku Hg 724+ diffractometer and crystal data collection and refinement parameters are summarized in Table 1. The structures were solved by using direct methods and standard difference map techniques, and were refined by full-matrix least-squares procedures on F^2 with SHELXTL (Version 6.10).[45] These programs were accessed through the WINGX 1.70.01 crystallographic collective package. All non-hydrogen atoms were refined anisotropically unless they were disordered. Hydrogen atoms were fixed

geometrically and were not refined. CCDC-960053 (for **2**) and CCDC-979501 (for **4**).†

Magnetic susceptibility measurements

Variable temperature susceptibility measurements were carried out in the temperature range 5–300 K with an applied magnetic field of 0.1 T on ground polycrystalline samples of compounds **2** and **4** using a Quantum Design MPMS XL-5 SQUID magnetometer. The susceptibility data were corrected for the sample holders previously measured under the same conditions and for the diamagnetic contributions of the sample using tables of Pascal's constants.

Synthesis

3,3′-Bis[(2,4,6-trimethyl-phenylimino)-methyl]-[1,1′]biphenyl-2,2′-diol (H_2L^1). To a solution of 2,4,6-trimethylaniline (1.38 g, 10.2 mmol) in a mixed medium of benzene (*ca.* 25 mL) and ethanol (*ca.* 25 mL), 3,3′-diformyl-2,2′-dihdroxy-1,1′-biphenyl (0.826 g, 3.41 mmol) was added dropwise and the reaction mixture was refluxed for 10 hours. The volatiles were removed under a vacuum and the residue was washed with methanol (*ca.* 3 × 20 mL) to get the pure product (**1**) as a yellow solid (1.55 g, 96%). ^{1}H NMR ($CDCl_3$, 400 MHz, 25 °C): δ 13.51 (s, 2H, O$\underline{H}$), 8.39 (s, 2H, C$\underline{H}$N), 7.62 (dd, 2H, $^3J_{HH}$ = 8 Hz, $^4J_{HH}$ = 2 Hz, $C_6\underline{H}_3$), 7.35 (dd, 2H, $^3J_{HH}$ = 8 Hz, $^4J_{HH}$ = 2 Hz, $C_6\underline{H}_3$), 7.04 (t, 2H, $^3J_{HH}$ = 8H, $C_6\underline{H}_3$), 6.88 (s, 4H, 2(2,4,6-$C_6\underline{H}_2(CH_3)_3$)), 2.29 (s, 6H, 2(2,4,6-$C_6H_2(C\underline{H}_3)_3$)), 2.20 (s, 12H, 2(2,4,6-$C_6H_2(C\underline{H}_3)_3$)). $^{13}C\{^1H\}$ NMR ($CDCl_3$, 400 MHz, 25 °C): δ 167.1 ($\underline{C}$HN), 159.0 ($\underline{C}_6H_3$), 145.8 [2,4,6-$\underline{C}_6H_2(CH_3)_3$], 135.5 [2,4,6-$\underline{C}_6H_2(CH_3)_3$], 134.6 ($\underline{C}_6H_3$), 132.1 [2,4,6-$\underline{C}_6H_2(CH_3)_3$], 129.2 [2,4,6-$\underline{C}_6H_2(CH_3)_3$], 128.5 ($\underline{C}_6H_3$), 125.8 ($\underline{C}_6H_3$), 119.3 ($\underline{C}_6H_3$), 118.6 ($\underline{C}_{10}H_5$), 20.9 [2,4,6-$C_6H_2(\underline{C}H_3)_3$], 18.7 [2,4,6-$C_6H_2(\underline{C}H_3)_3$]. IR data (KBr pellet) cm^{-1}: 3440(w), 2948(s), 2917(s), 1618(s), 1549(s), 1427(s), 1203(s), 1126(s), 745(w), 621(w), 556(w). HRMS (ES): *m*/*z* 477.2547 $[M + H]^+$, calcd 477.2537. Anal. calcd for $C_{32}H_{32}N_2O_2$: C, 80.64; H, 6.77; N, 5.88. Found: C, 80.80, H, 5.99; N, 5.92.

{Co[3,3′-bis-((R)-iminomethyl)-(1,1′)-biphenyl-2,2′-dioxo]}$_2$ (2). A solution of $Co(OAc)_2{\cdot}4H_2O$ (0.257 g, 1.03 mmol) in methanol (*ca.*: 25 mL) was added dropwise to a solution of 3,3′-bis[(2,4,6-trimethyl-phenylimino)-methyl]-[1,1′]biphenyl-2,2′-diol (**1**) (0.250 g, 0.525 mmol) in methanol (*ca.*: 20 mL). The resulting solution was refluxed for 6 hours. The reaction mixture was then cooled to room temperature and filtered and the filtrate was collected. The volatiles were removed under a vacuum to get a residue which was then dissolved in CH_2Cl_2 (*ca.*: 20 mL) and filtered. Finally, the volatiles were removed under a vacuum to get the product (**2**) as a red powder (0.123 g, 22%). IR data (KBr pellet) cm^{-1}: 3446(s), 2919(s), 2853(m), 1706(w), 1599(s), 1541(s), 1543(s), 1421(s), 1143(s), 1016(w), 1071(s), 852(s), 750(w), 621(w), 465(m). HRMS (ES): *m*/*z* 1067.3346 $[M]^+$, calcd 1067.3351. Anal. calcd for $C_{64}H_{60}Co_2N_4O_4$: C, 72.04; H, 5.67; N, 5.25. Found:, C, 72.10; H, 5.59; N, 5.32%.

3,3′-Bis[(2,4,6-trimethyl-phenylimino)-methyl]-[1,1′]binaphthalenyl-2,2′-diol (H_2L^2). To a solution of 2,4,6-trimethylaniline (0.982 g, 7.26 mmol) in a mixed medium of benzene (*ca.* 25 mL) and ethanol (*ca.* 25 mL), 3,3′-diformyl-2,2′-dihdroxy-1,1′-binaphthyl (0.825 g, 2.41 mmol) was added dropwise and the reaction mixture was refluxed for 10 hours. The volatiles were removed under a vacuum and the residue was washed with methanol (*ca.* 3 × 20 mL) to get the pure product (**3**) as a yellow solid (0.915 g, 68%). ^{1}H NMR ($CDCl_3$, 500 MHz, 25 °C): δ 12.94 (s, 2H, 2O$\underline{H}$), 8.64 (s, 2H, 2C$\underline{H}$N), 8.08 (s, 2H, 2$C_{10}\underline{H}_5$), 7.94 (d, 2H, $^3J_{HH}$ = 8 Hz, 2$C_{10}\underline{H}_5$), 7.39–7.35 (m, 6H, 2$C_{10}\underline{H}_5$), 6.95 (s, 4H, 2(2,4,6-$C_6\underline{H}_2(CH_3)_3$), 2.32 (s, 6H, 2[2,4,6-$C_6H_2(C\underline{H}_3)_3$], 2.25 (s, 12H, 2[2,4,6-$C_6H_2(C\underline{H}_3)_3$]. $^{13}C\{^1H\}$ NMR ($CDCl_3$, 400 MHz, 25 °C): δ 167.0 ($\underline{C}$HN), 154.9 ($\underline{C}_{10}H_5$), 145.9 (2,4,6-$\underline{C}_6H_2(CH_3)_3$), 135.8 ($\underline{C}_{10}H_5$), 134.8 [2,4,6-$\underline{C}_6H_2(CH_3)_3$], 129.3 ($\underline{C}_{10}H_5$), 129.2 ($\underline{C}_{10}H_5$), 128.9 [2,4,6-$\underline{C}_6H_2(CH_3)_3$], 128.6 (2$\underline{C}_{10}H_5$), 127.8 [2,4,6-$\underline{C}_6H_2(CH_3)_3$], 125.2 ($\underline{C}_{10}H_5$), 123.8 ($\underline{C}_{10}H_5$), 121.2 ($\underline{C}_{10}H_5$), 116.9 ($\underline{C}_{10}H_5$), 20.7 [2,4,6-$C_6H_2(\underline{C}H_3)_3$], 18.8 [2,4,6-$C_6H_2(\underline{C}H_3)_3$]. IR data (KBr pellet) cm^{-1}: 3386(s), 3474(s), 2921(s), 2853(w), 2652(w), 1693(w), 1623(s), 1502(w), 1449(s), 1144(m), 1336(s), 1117(s), 854(s), 748(m). HRMS (ES): *m*/*z* 577.2871 $[M + H]^+$, calcd 577.2855. Anal. calcd for $C_{40}H_{36}N_2O_2{\cdot}C_2H_5OH$: C, 81.00; H, 6.80; N, 4.50. Found: C, 80.66, H, 6.64; N, 4.52%.

{Co[3,3′-bis-((R)-iminomethyl)-(1,1′)-binaphthalenyl-2,2′-dioxo]}$_2$ (4). A solution of $Co(OAc)_2{\cdot}4H_2O$ (0.216 g, 0.867 mmol) in methanol (*ca.*: 25 mL) was added dropwise to a solution of 3,3′-bis[(2,4,6-trimethyl-phenylimino)-methyl]-[1,1′]binaphthalenyl-2,2′-diol (**3**) (0.250 g, 0.433 mmol) in methanol (*ca.*: 20 mL). The resulting solution was refluxed for 6 hours. The reaction mixture was then cooled to room temperature and filtered and the filtrate was collected. The volatiles were removed under a vacuum to get a residue which was then dissolved in CH_2Cl_2 (*ca.*: 20 mL) and filtered. Finally, the volatiles were removed under a vacuum to get the product (**2**) as a red powder (0.110 g, 20%). IR data (KBr pellet) cm^{-1}: 3451(s), 3474(m), 2918(s), 2854(w), 1623(s), 1503(w), 1356(m), 1173(m), 1144(m), 1117(s), 853(m), 748(s), 718(w), 465(w). HRMS (ES): *m*/*z* 1267.3977 $[M]^+$, calcd 1267.3937. Anal. calcd for $C_{80}H_{60}CoN_4O_4$: C, 75.82; H, 5.41; N, 4.42. Found:, C, 76.54; H, 5.92; N, 4.88%.

General procedure for the β-enaminone reaction of ketones and amines as catalyzed by the dinuclear $[CoL^1]_2$ (2) and $[CoL_2]_2$ (4) complexes

In a typical catalysis run performed at room temperature a vial was charged with a mixture of ketone : amine in a molar ratio of 1 : 4. A dinuclear cobalt complex (**2**/**4**) (0.01 mmol, 1 mol%) in *ca.* 0.5 mL THF was added to the mixture followed by THF (*ca.* 2 mL) and the resultant solution was stirred at room temperature for 6 hours. The volatiles were then removed *in vacuo* and the crude product was purified by column chromatography using silica gel as a stationary phase and eluting with a mixed medium of petroleum ether : EtOAc (v/v 60 : 40–97 : 3) to give the β-enaminone products (**5–14**) as a colourless liquid.

Procedure for the blank experiment

In a typical catalysis run a vial was charged with a mixture of acetyl acetone (0.100 g, 1.00 mmol) and methyl amine (0.311 g, 4.00 mmol) followed by THF (*ca.* 2.5 mL) and the resultant solution was stirred at room temperature for 6 hours. The volatiles were then removed *in vacuo* and the crude product was purified by column chromatography using silica gel as a

stationary phase and eluting with a mixed medium of petroleum ether : EtOAc (v/v 60 : 40) to give 4-(methylamino)pent-3-en-2-one (**5**) as a colorless liquid.

Procedure for the control experiment

In a typical catalysis run a vial was charged with a mixture of acetyl acetone (0.100 g, 1.00 mmol) and methyl amine (0.311 g, 4.00 mmol). The $Co(OAc)_2{\cdot}4H_2O$ complex (0.0049 g, 0.02 mmol, 2 mol%) in *ca.* 0.5 mL THF was added to the mixture followed by THF (*ca.* 2 mL) and the resultant solution was stirred at room temperature for 6 hours. The volatiles were then removed *in vacuo* and the crude product was purified by column chromatography using silica gel as a stationary phase and eluting with a mixed medium of petroleum ether:EtOAc (v/v 60 : 40) to give 4-(methylamino)pent-3-en-2-one (**5**) as a colourless liquid.

4-(Methylamino)pent-3-en-2-one (5)[55]

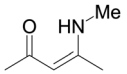

(**5**)

^{1}H NMR ($CDCl_3$, 400 MHz, 25 °C): δ 10.7 (b, 1H, $CH_3COCHC(N\underline{H}CH_3)(CH_3)$), 4.96 (s, 1H, $CH_3COC\underline{H}C(NHCH_3)(CH_3)$), 2.92 (d, 3H, $^3J_{HH}$ = 6 Hz, $CH_3COCHC(NHC\underline{H}_3)(CH_3)$), 1.98 (s, 3H, $C\underline{H}_3COCHC(NHCH_3)(CH_3)$), 1.90 (s, 3H, $CH_3COCHC(NHCH_3)(C\underline{H}_3)$). $^{13}C\{^1H\}$ NMR ($CDCl_3$, 125 MHz, 25 °C): δ 195.0 ($CH_3\underline{C}OCHC(NHCH_3)(CH_3)$), 164.4 ($CH_3COCH\underline{C}(NHCH_3)(CH_3)$), 95.4 ($CH_3CO\underline{C}HC(NHCH_3)(CH_3)$), 29.7 ($CH_3COCHC(NH\underline{C}H_3)(CH_3)$), 28.9 ($\underline{C}H_3COCHC(NHCH_3)(CH_3)$), 18.9 ($CH_3COCHC(NHCH_3)(\underline{C}H_3)$). GC-MS (ESI): m/z = 113 $[M]^+$. Anal. calcd for $C_6H_{11}NO$: C, 63.69; H, 9.80; N, 12.38; found: C, 63.64; H, 9.17; N, 12.35%.

4-(Ethylamino)pent-3-en-2-one (6)[55]

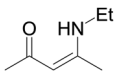

(**6**)

^{1}H NMR ($CDCl_3$, 400 MHz, 25 °C): δ 10.74 (b, 1H, $CH_3COCHC(N\underline{H}CH_2CH_3)(CH_3)$), 4.94 (s, 1H, $CH_3COC\underline{H}C(NHCH_2CH_3)(CH_3)$), 3.30–3.23 (m, 2H, $CH_3COCHC(NHC\underline{H}_2CH_3)(CH_3)$), 1.98 (s, 3H, $C\underline{H}_3COCHC(NHCH_2CH_3)(CH_3)$), 1.90 (s, 3H, $CH_3COCHC(NHCH_2CH_3)(C\underline{H}_3)$), 1.22 (t, 3H, $^3J_{HH}$ = 7 Hz, $CH_3COCHC(NHCH_2C\underline{H}_3)(CH_3)$). $^{13}C\{^1H\}$ NMR ($CDCl_3$, 100 MHz, 25 °C): δ 195.0 ($CH_3\underline{C}OCHC(NHCH_2CH_3)(CH_3)$), 163.3 ($CH_3COCH\underline{C}(NHCH_2CH_3)(CH_3)$), 95.2 ($CH_3CO\underline{C}HC(NHCH_2CH_3)(CH_3)$), 37.9 ($CH_3COCHC(NH\underline{C}H_2CH_3)(CH_3)$), 28.9 ($\underline{C}H_3COCHC(NHCH_2CH_3)(CH_3)$), 18.9 ($CH_3COCHC(NHCH_2CH_3)(\underline{C}H_3)$), 15.6 ($CH_3COCHC(NHCH_2\underline{C}H_3)(CH_3)$). GC-MS (ESI): m/z = 127 $[M]^+$.

4-(*n*-Propylamino)pent-3-en-2-one (7)[55]

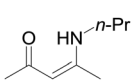

(**7**)

^{1}H NMR ($CDCl_3$, 400 MHz, 25 °C): δ 10.85 (b, 1H, $CH_3COCHC(N\underline{H}CH_2CH_2CH_3)(CH_3)$), 4.94 (s, 1H, $CH_3COC\underline{H}C(NHCH_2CH_2CH_3)(CH_3)$), 3.18 (quat, 2H, $CH_3COCHC(NHC\underline{H}_2CH_2CH_3)(CH_3)$), 1.98 (s, 3H, $C\underline{H}_3COCHC(NHCH_2CH_2CH_3)(CH_3)$), 1.90 (s, 3H, $CH_3COCHC(NHCH_2CH_2CH_3)(C\underline{H}_3)$), 1.64–1.55 (m, 2H, $CH_3COCHC(NHCH_2C\underline{H}_2CH_3)(CH_3)$), 0.96 (t, 3H, $^3J_{HH}$ = 7 Hz, $CH_3COCHC(NHCH_2CH_2C\underline{H}_3)(CH_3)$). $^{13}C\{^1H\}$ NMR ($CDCl_3$, 100 MHz, 25 °C): δ 194.6 ($CH_3\underline{C}OCHC(NHCH_2CH_2CH_3)(CH_3)$), 163.2 ($CH_3COCH\underline{C}(NHCH_2CH_2CH_3)(CH_3)$), 95.0 ($CH_3CO\underline{C}HC(NHCH_2CH_2CH_3)(CH_3)$), 44.7 ($CH_3COCHC(NH\underline{C}H_2CH_2CH_3)(CH_3)$), 28.7 ($\underline{C}H_3COCHC(NHCH_2CH_2CH_3)(CH_3)$), 23.4 ($CH_3COCHC(NHCH_2\underline{C}H_2CH_3)(CH_3)$), 18.8 ($CH_3COCHC(NHCH_2CH_2CH_3)(\underline{C}H_3)$), 11.4 ($CH_3COCHC(NHCH_2CH_2\underline{C}H_3)(CH_3)$). GC-MS (ESI): m/z = 141 $[M]^+$.

4-(i-Propylamino)pent-3-en-2-one (8)[55]

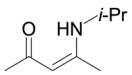

(**8**)

^{1}H NMR ($CDCl_3$, 400 MHz, 25 °C): δ 10.80 (b, 1H, $CH_3COCHC(N\underline{H}\{CH(CH_3)_2\})(CH_3)$), 4.88 (s, 1H, $CH_3COC\underline{H}C(NH\{CH(CH_3)_2\})(CH_3)$), 3.75–3.66 (m, 1H, $CH_3COCHC(NH\{C\underline{H}(CH_3)_2\})(CH_3)$), 1.96 (s, 3H, $C\underline{H}_3COCHC(NH\{CH(CH_3)_2\})(CH_3)$), 1.92 (s, 3H, $CH_3COCHC(NH\{CH(CH_3)_2\})(C\underline{H}_3)$), 1.21 (d, 6H, $^3J_{HH}$ = 6 Hz, $CH_3COCHC(NH\{CH(C\underline{H}_3)_2\})(CH_3)$). $^{13}C\{^1H\}$ NMR ($CDCl_3$, 100 MHz, 25 °C): δ 194.7 ($CH_3\underline{C}OCHC(NH\{CH(CH_3)_2\})(CH_3)$), 162.1 ($CH_3COCH\underline{C}(NH\{CH(CH_3)_2\})(CH_3)$), 95.1 ($CH_3CO\underline{C}HC(NH\{CH(CH_3)_2\})(CH_3)$), 44.9 ($CH_3COCHC(NH\{\underline{C}H(CH_3)_2\})(CH_3)$), 28.9 ($\underline{C}H_3COCHC(NH\{CH(CH_3)_2\})(CH_3)$), 24.0 ($CH_3COCHC(NH\{CH(\underline{C}H_3)_2\})(CH_3)$), 18.8 ($CH_3COCHC(NH\{CH(CH_3)_2\})(\underline{C}H_3)$). GC-MS (ESI): m/z = 141 $[M]^+$.

4-(*n*-Butylamino)pent-3-en-2-one (9)[55]

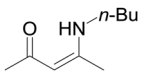

(**9**)

^{1}H NMR ($CDCl_3$, 400 MHz, 25 °C): δ 10.84 (b, 1H, $CH_3COCHC(N\underline{H}CH_2CH_2CH_2CH_3)(CH_3)$), 4.92 (s, 1H, $CH_3COC\underline{H}C(NHCH_2CH_2CH_2CH_3)(CH_3)$), 3.21 (quat, 2H, $^3J_{HH}$ = 7 Hz, $CH_3COCHC(NHC\underline{H}_2CH_2CH_2CH_3)(CH_3)$), 1.97 (s, 3H, $C\underline{H}_3COCHC(NHCH_2CH_2CH_2CH_3)(CH_3)$), 1.89 (s, 3H, $CH_3COCHC(NHCH_2CH_2CH_2CH_3)(C\underline{H}_3)$), 1.58–1.51 (m, 2H, $CH_3COCHC(NHCH_2C\underline{H}_2CH_2CH_3)(CH_3)$), 1.43–1.34 (m, 2H, $CH_3COCHC(NHCH_2CH_2C\underline{H}_2CH_3)(CH_3)$), 0.91 (t, 3H, $^3J_{HH}$ = 7 Hz, $CH_3COCHC(NHCH_2CH_2CH_2C\underline{H}_3)(CH_3)$). $^{13}C\{^1H\}$ NMR ($CDCl_3$, 100 MHz, 25 °C): δ 194.8 ($CH_3\underline{C}OCHC(NHCH_2CH_2CH_2CH_3)(CH_3)$), 163.4 ($CH_3COCH\underline{C}(NHCH_2CH_2CH_2CH_3)(CH_3)$), 95.2 ($CH_3CO\underline{C}HC(NHCH_2CH_2CH_2CH_3)(CH_3)$), 42.9 ($CH_3COCHC(NH\underline{C}H_2CH_2CH_2CH_3)(CH_3)$), 32.3 ($CH_3COCHC(NHCH_2\underline{C}H_2CH_2CH_3)(CH_3)$), 28.9 ($\underline{C}H_3COCHC(NHCH_2CH_2CH_2CH_3)(CH_3)$), 20.2 ($CH_3COCHC(NHCH_2CH_2\underline{C}H_2CH_3)(CH_3)$), 19.0 ($CH_3COCHC(NHCH_2CH_2CH_2CH_3)(\underline{C}H_3)$), 13.9 ($CH_3COCHC(NHCH_2CH_2CH_2\underline{C}H_3)(CH_3)$). GC–MS (ESI): m/z = 155 $[M]^+$.

4-((Pyridin-2-ylmethyl)amino)pent-3-en-2-one (10)[62]

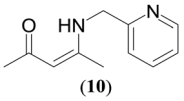

(**10**)

^{1}H NMR ($CDCl_3$, 400 MHz, 25 °C): δ 11.27 (b, 1H, $CH_3COCHC(N\underline{H}CH_2C_5H_4N)(CH_3)$), 8.54–8.53 (m, 1H,

$CH_3COCHC(NHCH_2C_5\underline{H}_4N)(CH_3)$), 7.68–7.63 (m, 1H, $CH_3COCHC(NHCH_2C_5\underline{H}_4N)(CH_3)$), 7.29–7.25 (d, 1H, $^3J_{HH}$ = 8 Hz, $CH_3COCHC(NHCH_2C_5\underline{H}_4N)(CH_3)$), 7.17 (t, 1H, $^3J_{HH}$ = 8 Hz, $CH_3COCHC(NHCH_2C_5\underline{H}_4N)(CH_3)$), 5.06 (s, 1H, $CH_3COC\underline{H}C(NHCH_2C_5H_4N)(CH_3)$), 4.57 (d, 2H, $^3J_{HH}$ = 7 Hz, $CH_3COCHC(NHC\underline{H}_2C_5H_4N)(CH_3)$), 2.01 (s, 3H, $C\underline{H}_3COCHC(NHCH_2C_5H_4N)(CH_3)$), 1.91 (s, 3H, $CH_3COCHC(NHCH_2C_5H_4N)(C\underline{H}_3)$). $^{13}C\{^1H\}$ NMR ($CDCl_3$, 100 MHz, 25 °C): δ 195.9 ($CH_3\underline{C}OCHC(NHCH_2C_5H_4N)(CH_3)$), 163.3 ($CH_3COCH\underline{C}(NHCH_2C_5H_4N)(CH_3)$), 157.9 ($CH_3COCHC(NHCH_2$-ipso-$\underline{C}_5H_4N)(CH_3)$), 149.7 ($CH_3COCHC(NHCH_2\underline{C}_5H_4N)(CH_3)$), 137.3 ($CH_3COCHC(NHCH_2\underline{C}_5H_4N)(CH_3)$), 122.6 ($CH_3COCHC(NHCH_2$-$\underline{C}_5H_4N)(CH_3)$), 121.0 ($CH_3COCHC(NHCH_2\underline{C}_5H_4N)(CH_3)$), 96.5 ($CH_3CO\underline{C}HC(NHCH_2C_5H_4N)(CH_3)$), 48.7 ($CH_3COCHC(NH\underline{C}H_2$-$C_5H_4N)(CH_3)$), 29.1 ($\underline{C}H_3COCHC(NHCH_2C_5H_4N)(CH_3)$), 19.2 ($CH_3COCHC(NHCH_2C_5H_4N)(\underline{C}H_3)$).

Ethyl 2-(ethylamino)cyclopent-1-ene-1-carboxylate (11)[62]

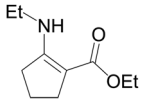

(11)

^1H NMR ($CDCl_3$, 400 MHz, 25 °C): δ 7.30 (b, 1H, $N\underline{H}CH_2CH_3$), 4.11 (quat, 2H, $^3J_{HH}$ = 7 Hz, $COOC\underline{H}_2CH_3$), 3.20 (pent, 2H, $^3J_{HH}$ = 7 Hz, $NHC\underline{H}_2CH_3$), 2.50 (pent, 4H, $^3J_{HH}$ = 8 Hz, $C\underline{H}_2CH_2C\underline{H}_2$), 1.83–1.76 (m, 2H, $CH_2C\underline{H}_2CH_2$), 1.24 (t, 3H, $^3J_{HH}$ = 7 Hz, $COOCH_2C\underline{H}_3$), 1.16 (t, 3H, $^3J_{HH}$ = 7 Hz, $NHCH_2C\underline{H}_3$). $^{13}C\{^1H\}$ NMR ($CDCl_3$, 100 MHz, 25 °C): δ 168.5 ($\underline{C}_5H_6$), 164.8 ($\underline{C}OOCH_2CH_3$), 92.1 ($\underline{C}_5H_6$), 58.4 ($COO\underline{C}H_2CH_3$), 39.3 ($NH\underline{C}H_2CH_3$), 31.9 (CH_2 of $\underline{C}_5H_6$), 28.9 (CH_2 of $\underline{C}_5H_6$), 20.9 (CH_2 of $\underline{C}_5H_6$), 16.2 ($NHCH_2\underline{C}H_3$), 14.8 ($COOCH_2\underline{C}H_3$). GC-MS (ESI): m/z = 183 $[M]^+$. Anal. calcd for $C_{10}H_{17}NO_2$: C, 65.54; H, 9.35; N, 7.64; found: C, 64.86; H, 9.16; N, 7.06%.

Ethyl 2-(*n*-propylamino)cyclopent-1-ene-1-carboxylate (12)[62]

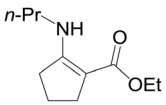

(12)

^1H NMR ($CDCl_3$, 400 MHz, 25 °C): δ 7.37 (b, 1H, $N\underline{H}CH_2CH_2CH_3$), 4.15 (quat, 2H, $^3J_{HH}$ = 7 Hz, $COOC\underline{H}_2CH_3$), 3.12 (quat, 2H, $^3J_{HH}$ = 7 Hz, $NHC\underline{H}_2CH_2CH_3$), 2.55–2.48 (m, 4H, $C\underline{H}_2CH_2C\underline{H}_2$), 1.81 (pent, 2H, $^3J_{HH}$ = 7 Hz, $CH_2C\underline{H}_2CH_2$), 1.59–1.50 (m, 2H, $NHCH_2C\underline{H}_2CH_3$), 1.24 (t, 3H, $^3J_{HH}$ = 7 Hz, $COOCH_2C\underline{H}_3$), 0.93 (t, 3H, $^3J_{HH}$ = 7 Hz, $NHCH_2CH_2C\underline{H}_3$). $^{13}C\{^1H\}$ NMR ($CDCl_3$, 100 MHz, 25 °C): δ 168.6 ($\underline{C}_5H_6$), 165.1 ($\underline{C}OOCH_2CH_3$), 92.1 ($\underline{C}_5H_6$), 58.4 ($COO\underline{C}H_2CH_3$), 46.4 ($NH\underline{C}H_2CH_2CH_3$), 32.0 ($CH_2$ of $\underline{C}_5H_6$), 29.0 (CH_2 of $\underline{C}_5H_6$), 24.2 ($NHCH_2\underline{C}H_2CH_3$), 21.0 ($CH_2$ of $\underline{C}_5H_6$), 14.8 ($COOCH_2\underline{C}H_3$), 11.3 ($NHCH_2CH_2\underline{C}H_3$). GC–MS (ESI): m/z = 197 $[M]^+$. Anal. calcd for $C_{11}H_{19}NO_2$: C, 66.97; H, 9.71; N, 7.10; found: C, 66.40; H, 10.07; N, 6.90%.

Ethyl 2-(i-propylamino)cyclopent-1-ene-1-carboxylate (13)[62]

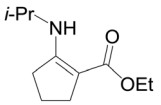

(13)

^1H NMR ($CDCl_3$, 400 MHz, 25 °C): δ 7.32 (b, 1H, $N\underline{H}CH(CH_3)_2$), 4.13 (quat, 2H, $^3J_{HH}$ = 7 Hz, $COOC\underline{H}_2CH_3$), 3.58–3.50 (m, 1H, $NHC\underline{H}(CH_3)_2$), 2.55 (t, 2H, $^3J_{HH}$ = 8 Hz, $C\underline{H}_2CH_2CH_2$), 2.48 (t, 2H, $^3J_{HH}$ = 8 Hz, $CH_2CH_2C\underline{H}_2$), 1.85–1.77 ($CH_2C\underline{H}_2CH_2$), 1.25 (t, 3H, $^3J_{HH}$ = 7 Hz, $COOCH_2C\underline{H}_3$), 1.18 (d, 6H, $^3J_{HH}$ = 7 Hz, $NHCH(C\underline{H}_3)_2$). $^{13}C\{^1H\}$ NMR ($CDCl_3$, 100 MHz, 25 °C): δ 168.6 ($\underline{C}_5H_6$), 164.0 ($\underline{C}OOCH_2CH_3$), 92.0 ($\underline{C}_5H_6$), 58.3 ($COO\underline{C}H_2CH_3$), 46.3 ($NH\underline{C}H(CH_3)_2$), 32.0 (CH_2 of $\underline{C}_5H_6$), 29.0 (CH_2 of $\underline{C}_5H_6$), 24.4 ($NHCH(\underline{C}H_3)_2$), 21.1 (CH_2 of $\underline{C}_5H_6$), 15.0 ($COOCH_2\underline{C}H_3$). GC-MS (ESI): m/z = 197 $[M]^+$. Anal. calcd for $C_{11}H_{19}NO_2$: C, 66.97; H, 9.71; N, 7.10; found: C, 66.29; H, 10.13; N, 6.87%.

Ethyl 2-(*n*-butylamino)cyclopent-1-ene-1-carboxylate (14)[62]

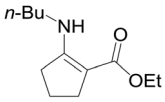

(14)

^1H NMR ($CDCl_3$, 400 MHz, 25 °C): δ 7.36 (b, 1H, $N\underline{H}CH_2CH_2CH_2CH_3$), 4.12 (quat, 2H, $^3J_{HH}$ = 7 Hz, $COOC\underline{H}_2CH_3$), 3.15 (quat, 2H, $^3J_{HH}$ = 7 Hz, $NHC\underline{H}_2CH_2CH_2CH_3$), 2.55–2.48 (m, 4H, $C\underline{H}_2CH_2C\underline{H}_2$), 1.81 (pent, 2H, $^3J_{HH}$ = 7 Hz, $CH_2C\underline{H}_2CH_2$), 1.54–1.47 (m, 2H, $NHCH_2C\underline{H}_2CH_2CH_3$), 1.41–1.32 (m, 2H, $NHCH_2CH_2C\underline{H}_2CH_3$), 1.25 (t, 3H, $^3J_{HH}$ = 8 Hz, $COOCH_2C\underline{H}_3$), 0.91 (t, 3H, $^3J_{HH}$ = 8 Hz, $NHCH_2CH_2CH_2C\underline{H}_3$). $^{13}C\{^1H\}$ NMR ($CDCl_3$, 100 MHz, 25 °C): δ 168.9 ($\underline{C}_5H_6$), 165.3 ($\underline{C}OOCH_2CH_3$), 92.3 ($\underline{C}_5H_6$), 58.6 ($COO\underline{C}H_2CH_3$), 44.6 ($NH\underline{C}H_2CH_2CH_2CH_3$), 33.3 ($CH_2$ of $\underline{C}_5H_6$), 32.3 ($NHCH_2\underline{C}H_2CH_2CH_3$), 29.3 ($CH_2$ of $\underline{C}_5H_6$), 21.2 (CH_2 of $\underline{C}_5H_6$), 20.2 ($NHCH_2CH_2\underline{C}H_2CH_3$), 15.1 ($COOCH_2\underline{C}H_3$), 14.0 ($NHCH_2CH_2CH_2\underline{C}H_3$). Anal. calcd for $C_{12}H_{21}NO_2$: C, 68.21; H, 10.02; N, 6.63; found: C, 67.42; H, 10.28; N, 6.50%.

Conflicts of interest

The authors declare no conflict of interest.

Acknowledgements

The authors would like to express their gratitude for the financial support from the Department of Science and Technology (EMR/2014/000254), New Delhi, India. We gratefully acknowledge the central Facility, Department of Chemistry, IIT Bombay, Mumbai, India, for the Single Crystal X-ray crystallographic characterization. We would also thank Professor P. Ghosh from Department of Chemistry, IIT Bombay, for his technical support, and Industrial Research and Consultancy Center (IRCC), IIT Bombay, for the Physical Property Measurement System.

References

1 S. Halder, S. Dey, C. Rizzoli and P. Roy, *Polyhedron*, 2014, **78**, 85–93.
2 D. Ruben, F. Nicolas, S. E. Carolina, V. Andrés, E. Albert, S. Mónica and M. Jorge, *New J. Chem.*, 2016, **40**, 6164–6170.
3 S. Jong Won, J. Ah Rim, L. Sun Young, K. Cheal, S. Hayami and K. S. Min, *Dalton Trans.*, 2016, **45**, 14089–14100.
4 A. J. Abdulghani and A. M. NooriKhaleel, *Bioinorg. Chem. Appl.*, 2013, 1–14.
5 R. M. Clarke and T. Storr, *Dalton Trans.*, 2014, **43**, 9380–9391.
6 X. Gong, Y. Y. Ge, M. Fang, Z. G. Gu, S. R. Zheng, W. S. Li, S. J. Hu, S. Li. Bin and Y. P. Cai, *CrystEngComm*, 2011, **13**, 6911–6915.
7 A. A. Khandar, K. Kirschbaum, M. Abedi, K. Mock, G. Tracy and V. Spasojevic, *New J. Chem.*, 2015, **39**, 2822–2831.
8 A. J. Rebecca, A. A. Hadi, X. Shengchang and G. T. Musie, *Inorg. Chim. Acta*, 2013, **394**, 220–228.
9 T. C. Davenport and T. D. Tilley, *Dalton Trans.*, 2015, **44**, 12244–12255.
10 E. P. DiMauro and M. C. Kozlowski, *Organometallics*, 2002, **21**, 1454–1461.
11 I. Bratko and M. Gómez, *Dalton Trans.*, 2013, **42**, 10664–10681.
12 S. Matsunaga and M. Shibasaki, *Chem. Commun.*, 2014, **50**, 1044–1057.
13 H. Shimakoshi, S. Hirose, M. Ohba, T. Shiga, H. Okawa and Y. Hisaeda, *Bull. Chem. Soc. Jpn.*, 2005, **78**, 1040–1046.
14 J. M. Jedrzejas and P. Setlow, *Chem. Rev.*, 2001, **101**, 607–618.
15 L. A. Gavrilova, C. J. Qin, R. D. Sommer, A. L. Rheingold and B. Bosnich, *J. Am. Chem. Soc.*, 2002, **124**, 1714–1722.
16 A. A. Khandar, J. White, T. Taghvaee-Yazdeli, S. A. Hosseini-Yazdi and P. McArdle, *Inorg. Chim. Acta*, 2013, **400**, 203–209.
17 A. Huber, L. Müller, H. Elias, R. Klement and M. Valko, *Eur. J. Inorg. Chem.*, 2005, 1459–1467.
18 H. Sakiyama, T. Suzuki, K. Ono, R. Ito, Y. Watanabe, M. Yamasaki and M. Mikuriya, *Inorg. Chim. Acta*, 2005, **358**, 1897–1903.
19 X. Li, L. Chen, L. Gao, Y. Zhang, S. F. Akogun and W. Dong, *RSC Adv.*, 2017, 35905–35916.
20 G. Ambrosi, M. Formica, V. Fusi, L. Giorgi, A. Guerri, M. Micheloni, P. Paoli, R. Pontellini and P. Rossi, *Inorg. Chem.*, 2007, **46**, 309–320.
21 S. K. Pandey, *Synlett*, 2006, 3366–3367.
22 Z. H. Zhang and J. Y. Hu, *J. Braz. Chem. Soc.*, 2006, **17**, 1447–1451.
23 Y. I. Cho, M. L. Ward and M. J. Rose, *Dalton Trans.*, 2016, **45**, 13466–13476.
24 C. L. Feng, N. N. Chu, S. G. Zhang, J. Cai, J. Q. Chen, H. Y. Hu and M. Ji, *Chem. Pap.*, 2014, **68**, 1097–1103.
25 M. Zhang, A. Abdukader, Y. Fu and C. Zhu, *Molecules*, 2012, **17**, 2812–2822.
26 Z. H. Zhang, Z. C. Ma and L. P. Mo, *Indian J. Chem.*, 2007, **46**, 535–539.
27 X. Chen, J. She, Z. C. Shang, J. Wu and P. Zhang, *Synth. Commun.*, 2009, **39**, 947–957.
28 Y. Zhao, J. Zhao, Y. Zhou, Z. Lei, L. Li and H. Zhang, *New J. Chem.*, 2005, **29**, 769–772.
29 H. Alokesh, D. K. Lakshmi, K. D. Ramakant, B. Antonio, A. Frontera and A. Ghosh, *Dalton Trans.*, 2015, **44**, 3862–3876.
30 F. Wodtke, R. F. Xavier, S. R. Mendes, A. R. M. D. Oliveira and R. A. A. Gariani, *Tetrahedron Lett.*, 2017, **58**, 231–234.
31 A. Thevenon, J. A. Garden, A. J. P. White and C. K. Williams, *Inorg. Chem.*, 2015, **54**, 11906–11915.
32 M. M. Pereira, M. J. F. Calvete, R. M. B. Carrilho and A. R. Abreu, *Chem. Rev.*, 2013, **42**, 6990–7027.
33 P. Ghorai, A. Chakraborty, A. Panja, T. K. Mondal and A. Saha, *RSC Adv.*, 2016, 36020–36030.
34 I. Ketata, L. Mechi, T. Ayed, T. Ben, M. Dusek, V. Petricek and R. Hassen, *Open J. Inorg. Chem.*, 2012, **02**, 33–39.
35 D. Kumar, A. Kumar and D. Dass, *Int. J. Inorg. Chem.*, 2013, 1–6.
36 Y. Guo, X. Hu, X. Zhang, X. Pu and Y. Wang, *RSC Adv.*, 2019, 41737–41744.
37 B. Ortiz and S. M. Park, *Bull. Korean Chem. Soc.*, 2000, **21**, 405–411.
38 L. Yang, D. R. Powell and R. P. Houser, *Dalton Trans.*, 2007, 955–964.
39 S. A. Carabineiro, L. C. Silva, P. T. Gomes, L. C. J. Pereira, L. F. Veiros, S. I. Pascu, M. T. Duarte, S. Namorado and R. T. Henriques, *Inorg. Chem.*, 2007, **46**, 6880–6890.
40 X. Song and X. Xue, *ACS Omega*, 2020, **5**, 8347–8354.
41 B. Moubaraki, S. Murray and C. Boskovic, *Dalton Trans.*, 2014, 2499–2511.
42 M. Murrie, *Chem. Soc. Rev.*, 2010, **39**, 1986–1995.
43 A. A. Khandar, K. Kirschbaum, M. Abedi, K. Mock, G. Tracy, V. Spasojevic and S. Hosseini-Yazdi, *New J. Chem.*, 2015, **39**, 2822–2831.
44 T. Kurahashi and U. H. Fujii, *Inorg. Chem.*, 2013, **52**, 3908–3919.
45 T. Hu, B. Zheng, X. Wang and X. Hao, *CrystEngComm*, 2015, **17**, 9348–9356.
46 M. J. Hossani, H. Yamasaki, M. Mikuriya, A. Kuribayashi and H. Sarkiyama, *Inorg. Chem.*, 2002, **41**(15), 4058–4062.
47 L. J. Daumann, P. Comba, J. A. Larrabee, G. chenk, R. Stranger, G. Cavigliasso and R. L. Gahan, *Inorg. Chem.*, 2013, **52**, 2029–2043.
48 B. Sarkar, S. M. I. Ray, M. G. B. Drew, A. Figuerola, C. Diaz and A. Ghosh, *Polyhedron*, 2006, **25**, 3084–3094.
49 D. K. Uttam, B. Julia, F. Candace, H. E. Sarah, P. F. Chad, D. N. Louise Petten, D. Andreas, K. M. Francesca and K. M. Christopher, *Dalton Trans.*, 2010, **39**, 5462–5477.
50 L. Zhang, W. Gao, Q. Wu, Q. Su, Z. Zhang and M. Ying, *J. Coord. Chem.*, 2013, **66**, 3182–3192.
51 G. V. Baryshnikov, B. F. Minaev, A. T. Baryshnikova and H. Ågren, *Chem. Phys.*, 2017, **491**, 48–55.
52 S. B. Govindh, S. B. Diwakar and Y. L. N. Murthy, *Org. Commun.*, 2012, **5**, 105–119.
53 B. Galloway, M. Royko, E. Sasmaz and B. Padak, *Chem. Eng. J.*, 2018, **336**, 253–262.
54 M. D. Argyle and C. H. Bartholomew, *Catalysts*, 2015, **5**, 145–269.

55 L. Rout, A. Kumar, R. S. Dhaka and P. Dash, *RSC Adv.*, 2016, **6**, 49923–49940.
56 U. K. Das, J. Bobak, C. Fowler, S. E. Hann, C. F. Petten, L. N. Dawe, A. Decken, M. Kerton and C. M. Kozak, *Dalton Trans.*, 2010, **39**, 5462–5477.
57 D. K. Suman and M. Arindam, *New J. Chem.*, 2014, **38**, 4985–4995.
58 J. M. Grill, J. H. Reibenspies and S. A. Miller, *J. Organomet. Chem.*, 2005, **690**, 3009–3017.
59 M. Villacampa and J. C. Mene, *Chem. Soc. Rev.*, 2014, 4633–4657.
60 Yu. N. Belokon, D. A. Chusov, T. V. Skrupskaya, D. A. Bor'kin, L. V. Yashkina, K. A. Lyssenko, M. M. Il'in, T. V. Strelkova, G. I. Timofeeva, A. S. Peregudov and M. North, *Russ. Chem. Bull.*, 2008, **57**, 1981–1988.
61 S. Takizawa, T. Katayama and H. Sasai, *Chem. Commun.*, 2008, 4113–4122.
62 D. H. Lee, S. E. Park, K. Cho, Y. Kim, T. Athar and I. M. Lee, *Tetrahedron Lett.*, 2007, **48**, 8281–8284.